

## Gate-controlled ZnO nanowires for field-emission device application

Seu Yi Li, Chia Ying Lee, Pang Lin, and Tseung Yuen Tseng

Citation: *Journal of Vacuum Science & Technology B* **24**, 147 (2006); doi: 10.1116/1.2151217

View online: <http://dx.doi.org/10.1116/1.2151217>

View Table of Contents: <http://scitation.aip.org/content/avs/journal/jvstb/24/1?ver=pdfcov>

Published by the AVS: Science & Technology of Materials, Interfaces, and Processing

---

### Articles you may be interested in

Erratum: "High-performance ZnO nanowire field effect transistors" [*Appl. Phys. Lett.* 89, 133113 (2006)]

*Appl. Phys. Lett.* **94**, 079902 (2009); 10.1063/1.2948901

Electron field emission from ZnO nanoparticles decorated on vertically aligned carbon nanotubes prepared by vapor-phase transport

*J. Vac. Sci. Technol. B* **26**, 1757 (2008); 10.1116/1.2975201

Effect of phosphorus dopant on photoluminescence and field-emission characteristics of Mg<sub>0.1</sub>Zn<sub>0.9</sub>O nanowires

*J. Appl. Phys.* **99**, 024303 (2006); 10.1063/1.2161420

Electrical properties of ZnO nanowire field effect transistors characterized with scanning probes

*Appl. Phys. Lett.* **86**, 032111 (2005); 10.1063/1.1851621

Depletion-mode ZnO nanowire field-effect transistor

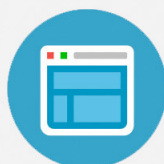
*Appl. Phys. Lett.* **85**, 2274 (2004); 10.1063/1.1794351

---



## Re-register for Table of Content Alerts

Create a profile.



Sign up today!



# Gate-controlled ZnO nanowires for field-emission device application

Seu Yi Li

*Institute and Department of Materials Science and Engineering, National Chiao Tung University, Hsinchu 30049, Taiwan*

Chia Ying Lee

*Department of Electronics Engineering and Institute of Electronics, National Chiao Tung University, Hsinchu 30050, Taiwan*

Pang Lin

*Institute and Department of Materials Science and Engineering, National Chiao Tung University, Hsinchu 30049, Taiwan*

Tseung Yuen Tseng<sup>a)</sup>

*Department of Electronics Engineering and Institute of Electronics, National Chiao Tung University, Hsinchu 30050, Taiwan and Department of Materials and Mineral Resources Engineering, National Taipei University of Technology, Taipei 10608, Taiwan*

(Received 21 June 2005; accepted 14 November 2005; published 17 January 2006)

Gate-controlled field-emission devices have great promise for a number of applications such as bright electron source or flat display array. The gate-controlled ZnO nanowire (NW) field-emission device was fabricated using lift-off fabrication process to synthesize side-gate control in the present investigation. This device effectively controls the turn-on electron beams and switches the drain current ( $I_d$ ) under a threshold gate voltage ( $V_T$ ) of  $\sim 35$  V. In the meantime, the current density of the device is  $\sim 1$  mA/cm<sup>2</sup> that is similar to carbon nanotube (CNT) field-emission level with a potential for the design of field-emission display (FED) devices. Furthermore, when the gate voltage ( $V_g$ ) is equal to 0 V, the turn-on electric field ( $E_{to}$ ) for ZnO NWs is  $\sim 0.8$  V/ $\mu$ m and the effective-field-enhancement factor  $\beta$  is  $\sim 7000$ . As  $V_g$  is increased to 10, 20, 30, and 40 V, the  $E_{to}$  lowers to the range of  $\sim 0.8$ – $0.6$  V/ $\mu$ m and the  $\beta$  value increases to  $\sim 7600$ – $17\,800$ . The continuous increases in  $V_g$  lowers the turn-on electric field because the local electric field ( $E_{local}$ ) generated induces an extra force that enhances electron emission from the ZnO NWs. Besides, the transconductance ( $g_m$ ) value can approach 0.388 mS while the  $V_g$  is increased to 44.5 V. The devices have well-controlled behavior and exhibit better Fowler-Nordheim characteristic in comparison with classic CNT field-emission devices. The gated ZnO NW array has a good opportunity to be applied to FED devices and be integrated to the semiconductor industry in the future. © 2006 American Vacuum Society. [DOI: 10.1116/1.2151217]

## I. INTRODUCTION

Recently, a class of triode structure has been suggested<sup>1–3</sup> for field-emission device application, which is called the side-gate-type triode field emitters where the gate electrodes are located around the cathode electrodes with a good gate dielectric oxide or isolation layers. Such a triode-type emitter has potential application in the flat display devices in the future. In the previous reports,<sup>4–6</sup> most of the triode-type field-emission devices (FEDs) were fabricated by a series of carbon-based materials such as carbon nanotubes (CNTs) or diamondlike carbon (DLC) films, which have good field-emission properties and good control over electron flow. Besides those materials, the field-emission characteristics<sup>7–9</sup> of some of the II–VI semiconductor nanostructures, especially two-dimensional (2D) nanostructure materials such as nanowires, nanobelts, or nanotetrapods, have also been investigated. The material ZnO is a II–VI semiconductor with  $\sim 60$  meV excited energy and  $\sim 3.47$ -eV-wide energy band

gap that has the attractive potential for nanoelectronics or nano-optical applications. Some ZnO nanowire (NW) fabrication methods or material properties were already presented in previous studies.<sup>10,11</sup> We have reported some results about the effect of processing conditions, such as dopant, substrate, and carrier gas, on the microstructure and field-emission properties of the ZnO NWs in a series of studies.<sup>12–14</sup> In this study, the one-step lift-off process was introduced to fabricate a side-gate-type-controlled ZnO NW field-emission device. The properties of the devices were also characterized and explained in terms of an existing theory.

## II. EXPERIMENT

The gate-controlled ZnO NW field-emission devices were fabricated through a procedure as shown in Fig. 1. The 200-nm-thick dry silicon dioxide SiO<sub>2</sub> was grown on *p*-type Si(100) substrate at  $\sim 1050$  °C. After the bottom electrode Pt was deposited, the isolation gate dielectric SiO<sub>2</sub> (500 nm) was synthesized on the top of Pt by plasma-enhanced chemical-vapor deposition (PECVD) process at 350 °C with the flow of gas mixture of O<sub>2</sub> and SiH<sub>4</sub> and the gate electrode

<sup>a)</sup>Author to whom correspondence should be addressed; electronic mail: tseng@cc.nctu.edu.tw

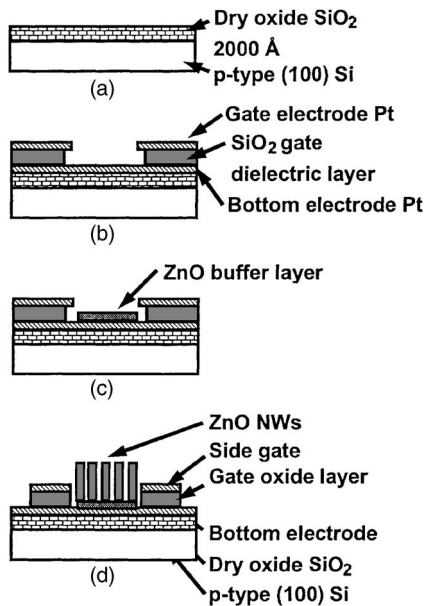


FIG. 1. Schematic description of the fabrication process for gate-controlled ZnO NW field-emission devices.

Pt was deposited on SiO<sub>2</sub> layer and postannealed at 350 °C for about 90 s. Then, we used etching process to define the region of the ZnO NW emitter. The 0.7 nm ultrathin (002) ZnO buffer layer was deposited using rf-sputter deposition under 10 mTorr Ar gas atmosphere on the Pt/SiO<sub>2</sub>/Si substrate which helps the vertical synthesis of ZnO NWs.<sup>15</sup> Finally, the 0.5 nm Au catalyst was sputter deposited in the patterns for which the width is ~50 μm and the lift-off process was used to remove the photoresist. The ZnO NWs were synthesized by vapor-liquid-solid (VLS) process at ~900 °C to complete the fabrication of this side-gate-controlled ZnO NW field-emission devices.

The field-emission properties of the gate-controlled ZnO NW field-emission devices were characterized in a high-vacuum measurement chamber with a base pressure of  $5.0 \times 10^{-8}$  Torr. The experimental setup for the measurement is shown in Fig. 2. The characteristics of the vertical field-effect transistor (FET) were measured by monitoring the

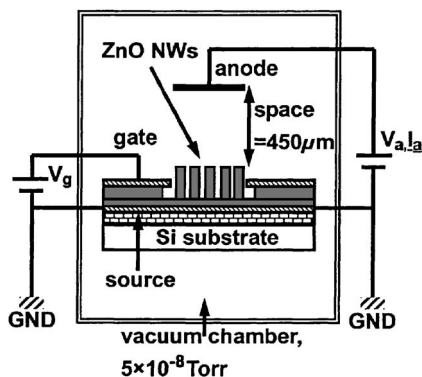


FIG. 2. Schematic diagram of a high-vacuum chamber system for field-emission property measurement.

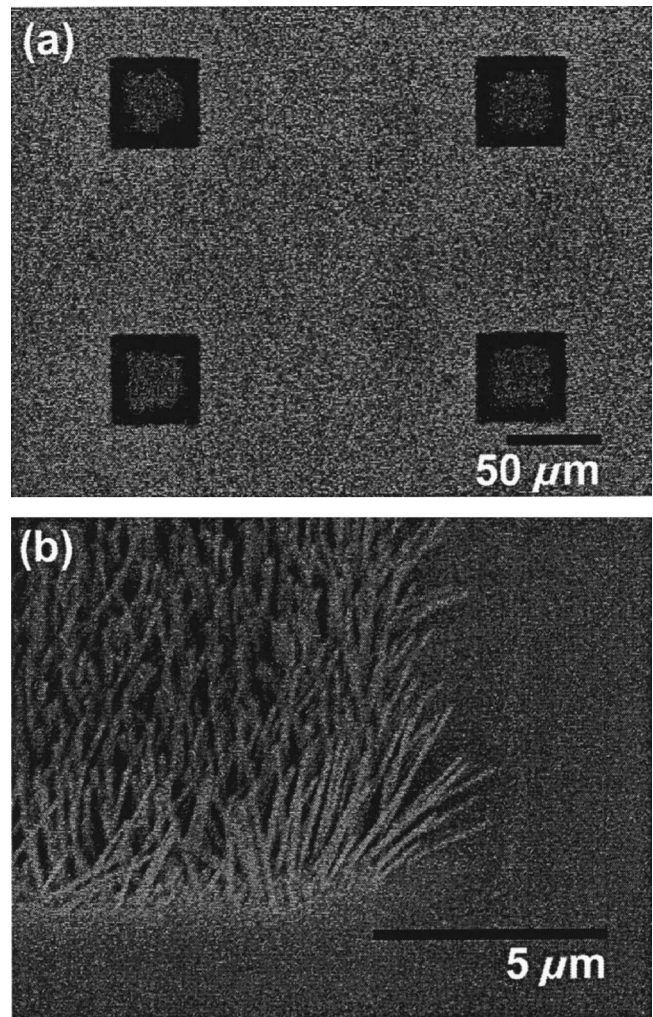


FIG. 3. SEM images of ZnO NWs synthesized on the emitter region of the triode. (a) An entire image for the four triode devices and (b) vertically grown ZnO NWs on the emitter region.

drain current ( $I_d$ ) as a function of the gate voltage ( $V_g$ ). An anode was made by Cu and was located at a distance of 450 μm above the ZnO NWs. The extra controlled voltage source offers the gate voltage sweep function which was measured by the variation of  $V_g$ . The anode current was measured as a function of extra controlled gate voltage and anode voltage, using Keithley 237 high-voltage source unit.

### III. RESULTS AND DISCUSSION

Figure 3 shows the field-emission scanning electron microscopy (FE-SEM, Hitachi S-4700I) images of the gate-controlled ZnO NW field-emission devices. The geometry of the device is shown in Fig. 3(a). The width of the square of ZnO NWs is ~50 μm and the space of each square pattern is 150 μm, which means that the half pitch is ~100 μm. The detailed nanostructure is shown in Fig. 3(b) of ZnO NWs. The ZnO buffer layer, which reduces the mismatch between ZnO NWs and Si substrate as reported elsewhere,<sup>15</sup> directs the growth of the (002) ZnO NWs vertically. These patterned ZnO NWs have uniform geometry that will help to enhance

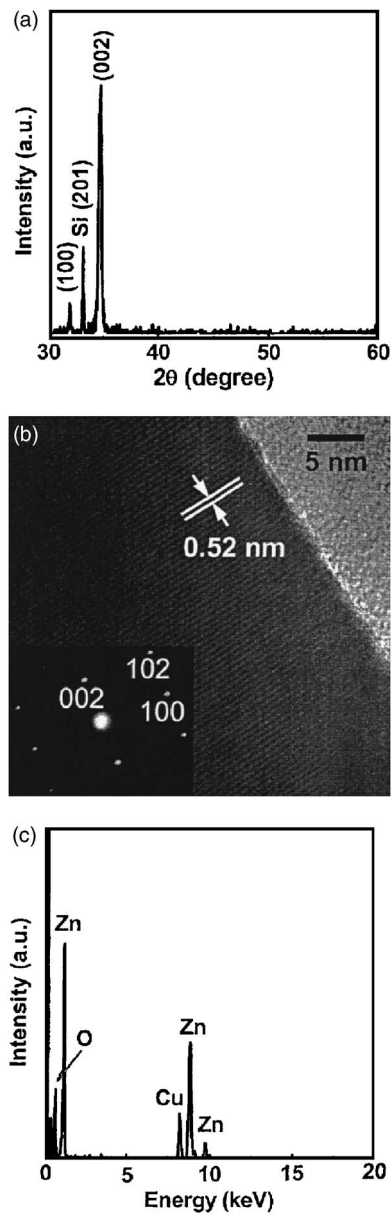


FIG. 4. Physical and chemical characterizations of the ZnO NWs. (a) XRD pattern of ZnO NWs, (b) HR-TEM image of the ZnO NWs and the inset shows SAED image, and (c) the EDS spectrum of the ZnO NWs.

the properties of field emission. The VLS-process-synthesized ZnO NWs are  $\sim 4 \mu\text{m}$  in length and  $\sim 50 \text{ nm}$  in width. The good crystallinity of ZnO NWs has been demonstrated by high-resolution transmission electron microscopy (HR-TEM) and x-ray diffraction analysis (XRD).

According to the XRD analysis shown in Fig. 4(a), the ZnO NWs have preferred orientation along the (002) direction. There are some weak peaks such as (100) and (110) which result from the lattice mismatch or unfavorable local growth during the VLS process. The full width at half maxima (FWHM) of the (002) ZnO NWs is  $\sim 0.145^\circ$  which means that the fabrication process is suitable for the vertically grown ZnO NWs which can be integrated for the design of the gate-controlled ZnO NW field-emission devices. The HR-TEM image indicated in Fig. 4(b) depicts that the

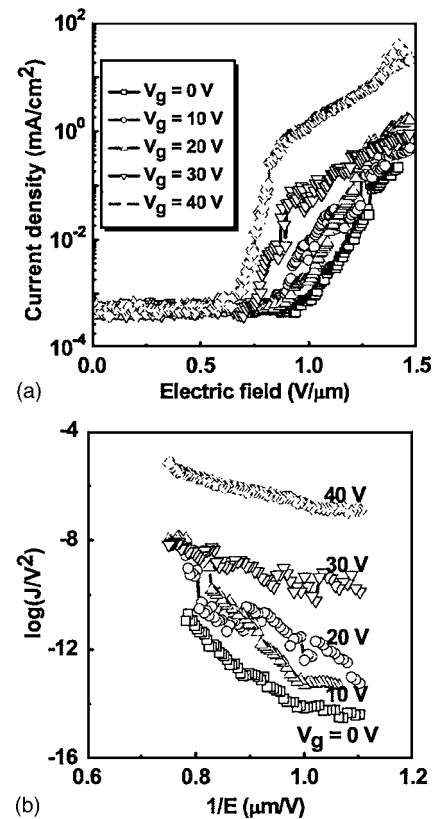


FIG. 5. Emission properties of the triode. (a) Relation of the current density vs electric field at various  $V_g$  indicated and (b) FN plot for various  $V_g$  indicated.

ZnO NWs have good crystallinity. The clear lattice fringes show that the  $d$  spacing of the (002)  $c$  axis is  $\sim 0.52 \text{ nm}$ , which is consistent with that of the International Center for Diffraction Data (ICDD-2000) database No. 80-0075 of ZnO. This image illustrates that the sidewall of ZnO NWs is smooth with fewer defects. The inset of Fig. 4(b) shows the selective area electron-diffraction (SAED) pattern along the (010) zone axis; the indexed spots present the well-crystallized ZnO NWs obtained using the VLS process. The energy dispersive spectrum (EDS) shown in Fig. 4(c) indicates the chemical composition of ZnO NWs. The Zn and O mole ratio is very close to 50/50 that demonstrates the negligible impurity in the ZnO NWs. Obviously, the VLS process offers good synthesis control and easy fabrication method for the gate-controlled ZnO NW field-emission devices.

The field-emission properties are measured by the field-emission measurement system, which is shown in Fig. 2. The reproducibility of the gate-controlled ZnO NW field-emission devices is verified by repeating the measurement on a number of samples. Typical field-emission property of the gate-controlled ZnO NW field-emission devices is shown in Fig. 5. Figure 5(a) depicts that the turn-on electric field of the gate-controlled ZnO NW field-emission device as a function of the gate voltages ( $V_g$ ) including 10, 20, 30, and 40 V, indicating that the turn-on electric field decreases from 0.95 to 0.63  $\text{V}/\mu\text{m}$  as a result of the extra electric field that the

TABLE I. Relationships among gate voltage ( $V_g$ ), turn-on electric field ( $E_{to}$ ), and effective-field-enhancement factor  $\beta$  of the gate-controlled ZnO NW field-emission devices.

| $V_g$ (V) | $E_{to}$ (V/ $\mu\text{m}$ ) | $\beta$ |
|-----------|------------------------------|---------|
| 0         | 0.92                         | 7 000   |
| 10        | 0.89                         | 7 300   |
| 20        | 0.84                         | 7 600   |
| 30        | 0.73                         | 16 400  |
| 40        | 0.58                         | 17 800  |

side gate induces while the  $V_g$  increases from 0 to 40 V. This phenomenon indicates that the extra electric field generated by  $V_g$  can help excite more electrons from the tips of ZnO NWs, leading to an increase in the turn-on current density and a decrease in the turn-on electric field. The field-emission characteristic that follows the Fowler-Nordheim (FN) equation can be written as

$$J = \frac{A\beta^2 E^2}{\phi} \exp\left(\frac{-B\phi^{3/2}}{\beta E}\right), \quad (1)$$

where  $J$  is the current density,  $E$  is the applied field,  $\phi$  is the work function of the emitter which is  $\sim 5.3$  eV for ZnO,  $\beta$  is the effective-field enhancement,  $A = 1.56 \times 10^{-10}$  A V $^{-2}$  eV, and  $B = 6.83 \times 10^3$  V eV $^{-3/2}$   $\mu\text{m}^{-1}$ . The FN plot shown in Fig. 5(b) depicts the effect of  $V_g$  on the turn-on electric properties of the gate-controlled ZnO NW field-emission devices. The total electric field ( $E_{\text{total}}$ ) comprises of two terms, namely, gate-induced electric field ( $E_{\text{gate}}$ ) and source-anode electric field ( $E_a$ ). The slope of each line on the FN plot is getting smaller with increasing  $V_g$ , which indicates that the effective-field-enhancement factor  $\beta$  becomes larger as listed in Table I. The  $\beta$  value increases from  $\sim 7000$  to  $\sim 17800$  when the  $V_g$  changes from 0 to 40 V. Therefore, the side gate can effectively switch this field-emission device under an optimized  $V_g \sim 37$  V. The gate-controlled properties of the ZnO NW field-emission devices are described below.

The side gate in this field-emission device plays an important role on terminal control, in which gate voltage ( $V_g$ ) introduces an extra electric field to focus or speed up the electrons emitted from the ZnO NW array. The electric field and turn-on current density as functions of  $V_g$  are shown in Fig. 6(b). While under the different turn-on electric field, the drain current ( $I_d$ ) versus gate voltage ( $V_g$ ) curves contain three regimes of interest. The regime of  $V_g$  from 5 to 35 V is called the gate leakage regime where  $I_d$  decreases with an increase in  $V_g$  because the emission current can be trapped by the side gate. The emission current transports through the isolating SiO $_2$ , resulting from space-charge-limited current flow, filled trap states in the depleted channel, and ohmic conduction through the substrate. The regime of  $V_g$  beyond 35 V but not exceeding 48 V, where the  $I_d$  increases rapidly with  $V_g$ , is called the field-emission excited regime. At this regime, the  $V_g$  tends to lower the energy barrier and leads to more electrons that easily tunnel from the tips of ZnO NWs to anode. The saturation regime exists at  $V_g$  higher than

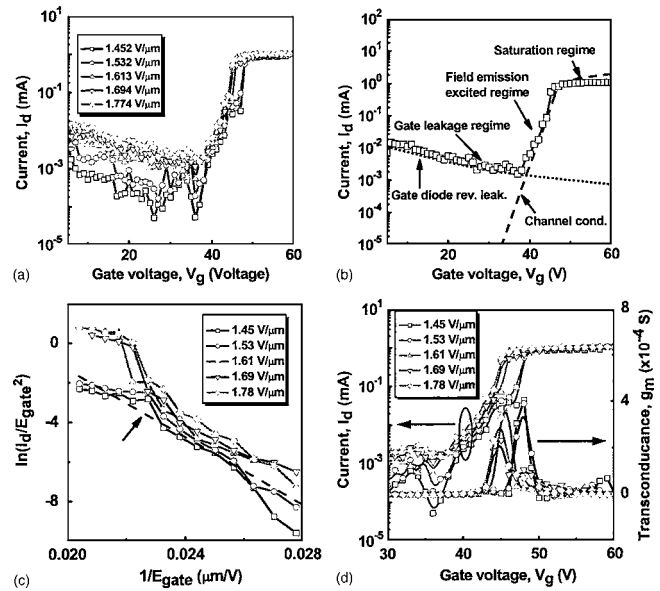


FIG. 6. (a) Plots of drain current  $I_d$  as a function of gate voltage  $V_g$  at various electric fields indicated. (b) Plot of  $I_d$  vs  $V_g$  emission device, (c) the FN plot for various electric fields indicated, and (d) curves of drain current and transconductance  $g_m$  as functions of gate voltage.

$\sim 50$  V in which the turn-on current reaches  $\sim 1.0$  mA/cm $^2$ . The channel gating above the threshold, the carrier density, and/or mean doping profile play an important role on the magnitude of the current. Based on  $I_d$ - $V_g$  plots as shown in the Fig. 6(b), the better stability of the emission current is obtained under a higher  $V_g$  ( $V_g > 35$  V) and corresponds to the higher turn-on electric field (e.g.,  $E_{\text{total}} > 1.61$  V/ $\mu\text{m}$ ). As shown in Fig. 6(a), the emission current of triode device could be controlled by both anode and gate voltages. Thus, our ZnO NW field-emission triode performs the better controllable ability than the only-gate voltage-controlling CNT field-emission triode reported in the previous paper.<sup>16</sup>

The FN plot [ $\ln(I/E^2)$  vs  $1/E$ ] at various  $V_g$  is shown in Fig. 6(c). The characteristic offset of each different applied electric field indicated in Fig. 6(c) presents the space-charge effect, which was widely observed in the semiconductor emitter located in high electric field.<sup>17</sup> In the low applied electric field below 1.61 V/ $\mu\text{m}$ , the linearity of the FN plot obeys the FN equation, which means that the FN tunneling mechanism dominates but the space-charge effect is a minor mechanism. On the other hand, the field-emission current decreases rapidly as indicated by the characteristic offset when the electric field is higher than 1.61 V/ $\mu\text{m}$ . The effects of space charge and of the series resistance are apparent from these curves, which are applicable to a large class of materials such as NWs. To avoid the space-charge effect, we need to apply a high-voltage ( $V_g > 20$  V), which can effectively decrease the induced space charges and limit the space-charge emission at the same time. While the space charges can be limited by  $V_g$ , the field emission of ZnO NWs could obey the FN relation and have better controlled properties.

To study the transconductance  $g_m$ , the relation of anode current ( $I_d$ ) as a function of gate voltage ( $V_g$ ) is presented in

Fig. 6(d). Each  $g_m$  curve for different turn-on electric fields has a unique maximum value, indicating the optimized  $V_g$  value for the control of the  $I_d$  current. In our study, at larger operating electric field beyond  $\sim 1.61$  V/ $\mu\text{m}$ ,  $V_g$  can induce higher focusing electric field which contributes to the decrease of  $g_m$  (0.388 mS) at small  $V_g$  equal to 44.5 V. But at low electric field of  $\sim 1.45$  V/ $\mu\text{m}$ , the maximum  $g_m$  (0.392 mS) can be achieved at  $V_g$  of  $\sim 48$  V. When the voltage drop from anode to cathode ( $V_{ds}$ ) is increased, the maximum  $g_m$  can be obtained at lower  $V_g$ . That is, the ZnO NWs can emit more stable current density under high  $V_{ds}$  and low  $V_g$ . The emission modulation can be obtained by controlling the gate voltage for our side-gate-controlled ZnO NW device. Therefore, the side-gate-controlled ZnO NW field-emission devices have better ability to control the electron flow at higher electric field from  $V_g$  which also let  $I_d$  become more stable.

#### IV. CONCLUSION

In summary, the gate-controlled ZnO NW field-emission devices have been successfully fabricated by a simple lift-off process. The VLS-processed ZnO NWs have good crystallinity and composition as demonstrated by TEM, XRD, and EDS analyses. The field-emission characteristics are improved under applied gate voltage ( $V_g$ ). At  $V_g$  of 35 V, the turn-on electric field is  $\sim 0.6$  V/ $\mu\text{m}$ , which is the best controlled condition for the device. Furthermore, the  $\beta$  value has been increased by the sweep of  $V_g$  because of the lower band energy level when  $V_g$  is applied so that electron tunneling is facilitated. The more electrons are emitted, the higher  $\beta$  value can be achieved. While  $V_g$  is equal to 40 V, the  $\beta$  value becomes  $\sim 17\,800$  which is larger than that of the  $\beta \sim 7000$  when  $V_g$  is equal to 0 V. The transconductance  $g_m$  is also an important factor to judge the ability of the gate-controlled ZnO NW field-emission devices. In our study, the  $g_m$  value is about  $4.0 \times 10^{-4}$  S, which means that the better

controlled  $V_g$  is located beyond  $\sim 35$  V. The side-gate-controlled ZnO NW field-emission devices have big potential to be applied in field-emission display (FED) in the future.

#### ACKNOWLEDGMENT

This work was supported by the National Science Council of R.O.C. under Contract No. NSC 93-2216-E-099-024.

- <sup>1</sup>I. T. Han, H. J. Kim, Y. J. Park, N. Lee, J. E. Jang, J. W. Kim, J. E. Jung, and J. M. Kim, *Appl. Phys. Lett.* **81**, 2070 (2002).
- <sup>2</sup>A. Wisitsora-At, W. P. Kang, J. L. Davidson, C. Li, D. V. Kerns, and M. Howell, *J. Vac. Sci. Technol. B* **21**, 1665 (2003).
- <sup>3</sup>Q. H. Wang, M. Yan, and R. P. H. Chang, *Appl. Phys. Lett.* **78**, 1294 (2000).
- <sup>4</sup>J. L. Davidson, W. P. Kang, and A. Wisitsora-At, *Diamond Relat. Mater.* **12**, 429 (2003).
- <sup>5</sup>C. Y. Hong and A. I. Akinwande, *J. Vac. Sci. Technol. B* **21**, 500 (2003).
- <sup>6</sup>Y. W. Jin, J. E. Jung, Y. J. Park, J. H. Choi, D. S. Jung, H. W. Lee, S. H. Park, N. S. Lee, J. M. Kim, T. Y. Ko, S. J. Lee, S. Y. Hwang, J. H. You, J. B. Yoo, and C. Y. Park, *J. Appl. Phys.* **92**, 1065 (2002).
- <sup>7</sup>Q. H. Li, Q. Wan, Y. J. Chen, T. H. Wang, H. B. Jia, and D. P. Yu, *Appl. Phys. Lett.* **85**, 636 (2004).
- <sup>8</sup>H. Z. Zhang, R. M. Wang, and Y. W. Zhu, *J. Appl. Phys.* **96**, 624 (2004).
- <sup>9</sup>Y. B. Li, Y. Bando, and D. Golberg, *Appl. Phys. Lett.* **84**, 3603 (2004).
- <sup>10</sup>S. Y. Bae, H. C. Choi, C. W. Na, and J. Park, *Appl. Phys. Lett.* **86**, 033102 (2005).
- <sup>11</sup>L. Wang, X. Zhang, S. Zhao, G. Zhou, Y. Zhou, and J. Qi, *Appl. Phys. Lett.* **86**, 024108 (2005).
- <sup>12</sup>S. Y. Li, P. Lin, C. Y. Lee, and T. Y. Tseng, *J. Appl. Phys.* **95**, 3711 (2004).
- <sup>13</sup>S. Y. Li, P. Lin, C. Y. Lee, and T. Y. Tseng, *J. Mater. Sci.: Mater. Electron.* **15**, 505 (2004).
- <sup>14</sup>S. Y. Li, P. Lin, C. Y. Lee, T. Y. Tseng, and C. J. Huang, *J. Phys. D* **37**, 2274 (2004).
- <sup>15</sup>S. Y. Li, C. Y. Lee, P. Lin, M. S. Ho, and T. Y. Tseng, *J. Nanosci. Nanotechnol.* **4**, 968 (2004).
- <sup>16</sup>I. T. Han, H. J. Kim, Y. J. Park, N. Lee, J. E. Jang, J. W. Kim, J. E. Jung, and J. M. Kim, *Appl. Phys. Lett.* **81**, 2070 (2002).
- <sup>17</sup>S. Johnson, A. Markwitz, M. Rudolphi, H. Baumann, S. P. Oei, B. K. Teo, and W. I. Milne, *Appl. Phys. Lett.* **85**, 3277 (2004).